Title

Fast neutron activation of ubiquitous materials

Authors

Lee, M

Norman, EB

Akindele, OA

et al.

Publication Date

2022-03-01

DOI

10.1016/j.apradiso.2022.110098

Applied Radiation and Isotopes 181 (2022) 110098

Contents lists available at ScienceDirect

Applied Radiation and Isotopes

journal homepage: www.elsevier.com/locate/apradiso

Fast neutron activation of ubiquitous materials

M. Lee [a,1], E.B. Norman [a,b,*], O.A. Akindele [a,2], K.J. Thomas [a,2], P.V. Guillaumon [c,3], J. L. Sabella [a], R.E. Meyer [a], H.A. Shugart [a,4]

[a] University of California Berkeley, CA, USA
[b] Lawrence Berkeley National Laboratory, Berkeley, CA, USA
[c] University of Sau Paulo, Sau Paulo, Brazil

A B S T R A C T

Nuclear explosions expose ubiquitous materials to large numbers of neutrons, producing a variety of radioactive isotopes. To simulate such phenomena from both fission and thermonuclear explosions, we irradiated 29 different targets with approximately 3 and 14 MeV neutrons and measured the beta-delayed gamma rays using germanium detectors. For each neutron energy, the expected radioisotopes, half-lives, and gamma ray energies were deduced. From measurements of the ratios of activities of the radionuclides produced by neutron irradiations, we were able to identify several materials that are particularly sensitive to the neutron energy spectra.

1. Introduction & motivation

An important analytic capability for nuclear forensics and security applications is the ability to determine the radiation signatures of both fission and thermonuclear type weapons. A number of previous studies demonstrated that observations of beta-delayed gamma rays from fission fragments can be used to distinguish fissions of ^{235}U from that of ^{239}Pu. Such measurements were also shown to provide information on the neutron energy spectra (Marrs et al. (2008); Iyengar et al. (2013); Swanberg et al. (2009); Beddingfield and Cecil (1998); Hollas et al. (1987)). Here we concentrate on another potential source of nuclear forensic information. Nuclear explosions can expose ubiquitous materials to large numbers of neutrons, ultimately producing a variety of radioactive isotopes. By identifying the radioactive species produced by neutron interactions and analyzing the data qualitatively and quantitatively, we can determine what signatures can provide information on the type of weapon that exploded.

In order to understand what radioisotopes are produced due to neutron activation, we first need to understand what and how the peak energies of the free neutrons are generated. Fission weapons rely on the fission of ^{235}U or ^{239}Pu and consequently produce an average of 2.5 neutrons that peak at energies of 2–3 MeV. Thermonuclear weapons combine both fusion and fission technology, using the fission to trigger a dt fusion reaction that produces 14 MeV neutrons. If either of these types of weapons were detonated, the high-energy free neutrons produced by these reactions will react with nuclei in the surroundings in four main ways: (n,γ), (n,p), (n,α), and (n,2n).

The radioactive nuclides produced will in turn undergo beta and gamma decays and could provide forensic clues to infer what type of nuclear weapon was used.

2. Methodology

Neutron activations with roughly 3- and 14- MeV neutrons were performed on 25 elemental targets and 4 additional targets using the 88 Inch Cyclotron at the Lawrence Berkeley National Laboratory. Neutrons were produced by bombarding a thick Be metal target with deuterons. A broad distribution of neutrons with peak energy approximately 3 MeV was produced using 6 MeV deuterons; 14 MeV with 30 MeV deuterons. Beam currents were approximately 500 nA for 6 MeV and 1 microAmp for 30 MeV. (Meulders et al. (1975).

The 29 targets we used were Ag, Al, Au, Cd, Co, Cu, Fe, Ga, Ge, Hf, In, Mn, Mo, Nb, Ni, Pb, Se, Sn, Ta, Ti, V, W, Y, Zn, Zr, stainless steel, and US coins: quarters, nickels, and dimes. Most of the targets were metal foils of various thicknesses approximately 2.54 x 2.54 cm in size and ranging in mass from 1.5 to 13 g. Targets were placed in air directly behind the

* Corresponding author. University of California Berkeley, CA, USA.
E-mail address: ebnorman@lbl.gov (E.B. Norman).
[1] Present address: University of North Carolina, Chapel Hill, NC, USA.
[2] Present Address: Lawrence Livermore National Laboratory, Livermore, CA, USA.
[3] Present address: Laboratori Nazionali del Gran Sasso, Assergi (L'Aquila), Italy.
[4] Deceased.

https://doi.org/10.1016/j.apradiso.2022.110098
Received 20 September 2021; Accepted 4 January 2022
Available online 11 January 2022

Be target for neutron irradiation and were irradiated for 10 minutes at 3 MeV and 3 minutes at 14 MeV, then counted with three high-purity germanium detectors for gammas emitted by the radioactive products.

In order to conduct this experiment on as many targets as possible, three detectors (labeled 1, 2, and 3) were used. These detectors were 50%, 60%, and 85% efficient respectively compared to a 7.6 x 7.6 cm NaI detector. The types of detectors and positions used to count the samples are shown in Table 1.

The length of measurement of each target varied depending on the in-tensity of the source, the position of the detector relative to the source, and the energies of the gammas. Gamma ray peaks were evaluated for the two neutron energies to identify differences in the radioactive species produced and in the initial activities of these products following irradiation.

Gamma ray counting was done starting approximately 30 minutes after irradiation and was done several times for each target over a period of several days. Each target was counted for approximately 10–20 minutes. Targets were placed at distances from the detectors ranging from 0.32 cm up to 29 cm to minimize deadtimes. Efficiency measurements were done at each distance using standard calibrated gamma ray sources. Measurement times and positions for each target varied in order to accommodate the variations in efficiencies of the detectors, the activities of the produced isotopes, as well as the half-life of the products. There were also additional constraints to measurement times due to the large number of samples and small number of detectors. Data was accumulated using ORTEC PC-based data acquisition systems.

3. Analysis

The main goal of the analysis was to find isotopes that are observable via gamma ray emission after a nuclear explosion and that provide information about the nature of the weapon. Each isotope has a unique half life and a Q value, or reaction threshold energy that we obtained from the National Nuclear Data Center (NNDC) website (Pritychenko and Sonzogni (2021)) and the Table of Radioactive Isotopes (Chu et al. (1999)). Using this information, we conducted qualitative analyses on what isotopes we would be able to observe depending on the energies of the neutrons. Isotopes with threshold energies larger than 3 MeV can only be produced during a thermonuclear explosion, while isotopes with thresholds less than 3 MeV will be produced in both pure fission and thermonuclear explosions. Materials that are po-tentially useful for this type of forensic investigation were selected based on their half lives and gamma-ray intensities.

We extracted peak areas for the prominent gammas observed at both 3 and 14 MeV neutron energy from each target material. Using this data, calculations of the initial activities of the isotopes produced at both neutron energies were conducted.

$$\text{Activity} = \frac{\text{Number of Counts}}{It \cdot \varepsilon \cdot b_\gamma} \tag{1}$$

Where lt is the live time of the measurements, ε is the detector efficiency at the gamma ray peak energy in question and b_γ is the branching ratio of that gamma ray.

Decay corrections were taken into account for the time between irradiation and counting and for decay during the counting period.

Table 1
Detector types and positions of the targets for each detector.

Detector 1	Detector 2	Detector 3
50% eff	60% eff	85% eff
P0: 0.64 cm	N/A	P0: 0.32 cm
P1: 3.2 cm	N/A	P1: 2.9 cm
P2: 8.3 cm	N/A	P2: 7.9 cm
P3: 18.4 cm	P3: 0.79 cm	P3: 18.4 cm
P4: 28.6 cm	P4: 11.0 cm	P4: 28.3 cm

$$A_0 = A_m \frac{\lambda \cdot \Delta t_r}{1 - e^{-\lambda \cdot \Delta t_r}} \cdot e^{-\lambda \cdot \Delta t} \tag{2}$$

A_0 is the activity at the end of bombardment, A_m is the activity at the beginning of measurement, λ is the decay constant, Δt_r is the real time of measurement and Δt is the time between the end of bombardment and beginning of measurement.

For most of the targets investigated, we found that for one or more reasons, they did not prove to be useful in distinguishing the nature of the nuclear explosion. For some, the half lives of the produced radionuclides were simply too short. For others the gamma ray intensities were too small. In others, the signatures observed from both 3 and 14 MeV irradiations were very similar. A list of the radioisotopes produced from all of the irradiated targets, their threshold energies, and half lives is shown in Table 2.

4. Results

In the end, eight of our target materials produced gamma-ray spectra that are clearly different for these two neutron energies: Ni, Ga, Ag, Au, US nickel, dime, and quarter coins, and stainless steel. Fig. 1 through 4 depict relevant portions of the gamma ray spectra of these neutron irradiated targets. The gamma-ray measurements at 3 and 14 MeV shown in these figures were conducted at the same time after both irradiations.

The ^{58}Ni(n,p)^{58}Co reaction has a Q-value of +0.401 MeV. Thus, the 811 keV gamma ray emitted in the decay of the ^{58}Co ($t_{1/2}$ = 70.9 days) was observed following both the 3 and 14 MeV irradiations. As can be seen in Fig. 1, at the higher neutron energy we also observed gammas at 122 and 136 keV from the decay of ^{57}Co ($t_{1/2}$ = 272 days) and at 127, (1378, 1758, and 1920 not shown) keV from ^{57}Ni ($t_{1/2}$ = 35.6 hours). These radioisotopes were produced by the ^{58}Ni(n,d) and ^{58}Ni(n,2n) reactions with threshold energies of 6.05 and 12.43 MeV, respectively.

United States nickel, dime, quarter, and half-dollar coins are made from alloys of nickel and copper (Mint (2021)). Similarly, many steels contain nickel that is added in order to prevent corrosion. This presence of nickel lead to our observations of ^{57}Co and ^{57}Ni gammas in the spectra collected from these materials following the 14-MeV irradiations.

Gallium is not a very common element, but it is used to stabilize the physical structure of plutonium metal used in some nuclear weapons (Hecker (2000)). Fig. 2 shows peaks in both the 3 and 14 MeV spectra at the energies of 438 keV and 834 keV emitted in the decay of ^{69m}Zn ($t_{1/2}$ = 13.8 h) produced via the ^{69}Ga (n,p) and ^{72}Ga ($t_{1/2}$ = 14.1 h) via the ^{71}Ga(n,γ) reactions, respectively. Although both 3 and 14 MeV neutrons produce these isotopes, they have different relative intensities at these two neutron energies. Using these spectra, we determined the relative intensities of the 438 keV and 834 keV gammas. The measured peak areas were corrected for 1) the different detector efficiencies at these two gamma energies and 2) the decay back to the end of irradiation, and 3) the slightly different emission probabilities of these two gamma rays. The efficiency at 438 keV is approximately 1.5 times larger than the efficiency at 834 keV for Detector 3. Considering all of these corrections, the ratios of activities at the end of bombardment are ^{69m}Zn/^{72}Ga = 0.24 ± 0.02 at 3 MeV (blue) and ^{69m}Zn/^{72}Ga = 1.9 ± 0.1 at 14 MeV (red).

The gammas labeled in Fig. 3 are emitted by the decay of ^{106m}Ag ($t_{1/2}$ = 8.28 days) produced from the (n,2n) reaction on ^{107}Ag. The reaction's threshold energy is 9.626 MeV and thus these gammas were only observed in the target irradiated with 14 MeV neutrons.

The ^{197}Au(n,2n)^{196}Au has a Q-value of −8.072 MeV. Thus, as seen in Fig. 4, the 333, 356, and 426 keV gamma rays emitted in the beta decay of the ^{196}Au ($t_{1/2}$ = 6.13 days) were observed only after the 14 MeV irradiation. We also observed the 412 keV gamma that is emitted in the decay of ^{198}Au ($t_{1/2}$ = 2.70 days) that is produced by the (n,γ) reaction.

Table 2
Targets and their Radioactive Products.

Target	Reaction	Radioactive Product	Half Life	Threshold Energy (MeV)
Ag	(n, 2n)	$^{Ag}106m$	8.28 d	9.63
Al	(n, γ)	$^{Al}28$	2.24 min	0
	(n,2n)	$^{Al}26$	7.17 x 10^5 yr	13.55
	(n,p)	$^{Mg}27$	9.46 min	1.90
	(n, α)	$^{Na}24$	15.0 h	3.250
Au	(n,γ)	$^{Au}198$	2.70 d	0
	(n,2n)	$^{Au}196$	6.18 d	8.114
	(n,α)	$^{Ir}194$	19.3 h	0
Cd	(n,p)	$^{Ag}110m$	250.0 d	2.128
	(n,p)	$^{Ag}112$	3.13 h	3.238
	(n,g)	Cd115	53.5 h	0
Co	(n, γ)	$^{Co}60$	5.27 yr	0
	(n,2n)	$^{Co}58$	70.9 d	10.633
	(n,p)	$^{Fe}59$	44.5 d	0.796
	(n, α)	$^{Mn}56$	2.58 h	0
Cr	(n, γ)	$^{Cr}51$	27.7 d	0
	(n,p)	$^{V}53$	1.61 min	3.255
Cu	(n, γ)	$^{Cu}64$	12.7 h	0
	(n,α)	$^{Co}60$	5.27 yr	0
	(n,p)	$^{Ni}65$	2.52 h	1376.7
	(n,α)	$^{Co}62$	1.50 min	0.196
	(n,α)	$^{Co}62m$	13.9 min	0.196
Fe	(n,2n)	$^{Fe}53$	8.51 min	13.629
	(n,p)	$^{Mn}54$	312 d	0
	(n, α)	$^{Cr}51$	27.7 d	0
	(n,p)	$^{Mn}56$	2.58 h	2965.7
Ga	(n, γ)	$^{Ga}70$	21.1 min	0
	(n,p)	$^{Zn}69m$	13.8 h	0.130
	(n,2n)	$^{Ga}68$	67.6 min	10.464
	(n,α)	$^{Cu}66$	5.12 min	0
	(n, γ)	$^{Ga}72$	14.1 h	0
	(n,p)	$^{Zn}71$	2.45 min	2.057
	(n,p)	$^{Zn}71m$	3.96 h	2.057
Ge	(n,2n)	$^{Ge}69$	39.1 h	11.699
	(n,p)	$^{Ga}72$	14.0 h	3.260
	(n,α)	$Zn69^{m}$	13.8 hr	0
	(n,p)	$^{Ga}73$	4.86 h	0.827
	(n,γ)	$^{Ge}75$	82.8 min	0
	(n,p)	$^{Ga}74$	8.12 min	4.653
	(n,γ)	$^{Ge}77$	11.3 h	0
Hf	(n,2n)	$^{Hf}178m2$	31 yr	6.133
In	(n,p)	$^{Cd}115$	53.7 h	0.675
	(n,α)	$^{Ag}112$	3.13 h	0
Mn	(n, γ)	$^{Mn}56$	2.58 h	0
	(n,2n)	$^{Mn}54$	312 d	10.414
Mo	(n,p)	$^{Nb}95$	35.0 d	0.145
	(n,p)	$^{Nb}96$	23.4 h	2.435
	(n,γ)	$^{Mo}99$	65.9 h	0
Nb	(n,2n)	$^{Nb}92m$	10.2 d	8.927
	(n,α)	Y90	3.19 h	0
Ni	(n,2n)	$^{Ni}57$	35.6 h	12.429
	(n,p)	$^{Co}58$	70.9 d	0
	(n,p)	$^{Co}60$	5.27 yr	2.075
	(n,d)	$^{Co}57$	272 d	6.051
Pb	(n, α)	$^{Hg}203$	46.6 d	0
	(n, p)	$^{Ti}208$	3.05 min	4.237
Se	(n,2n)	Sc_{44}	2.44 d	11.581
Sn	(n,p)	$^{In}117$	43.2 min	0.678
	(n,2n)	$^{Sn}117m$	13.6 d	9.406
Ta	(n,p)	$^{Hf}181$	42.4 d	0.255
	(n,α)	$^{Lu}178m$	23.1 min	0
Ti	(n,p)	$^{Sc}46$	83.8 d	1.619
	(n,p)	$^{Sc}47$	3.35 d	0
	(n,p)	$^{Sc}48$	43.7 h	3.274
	(n, γ)	$^{Ti}51$	5.76 min	0
V	(n, γ)	$^{V}52$	3.74 min	0
	(n,2n)	$^{V}50$	1.40 x 10^{17} yr	11.270
	(n,p)	$^{Ti}51$	5.76 min	1.722
	(n,α)	$^{Sc}48$	43.7 h	2.094
W	(n,p)	$^{Ta}184$	8.7 h	2.100
	(n,γ)	$^{W}187$	23.7 h	0

Table 2 (*continued*)

Target	Reaction	Radioactive Product	Half Life	Threshold Energy (MeV)
Y	(n,γ)	$^{Y}90m$	3.19 h	0
	(n,2n)	$^{Y}88$	107 d	11.610
Zn	(n, γ)	$^{Zn}65$	244 d	0
	(n,p)	$^{Cu}64$	12.7 h	0
	(n,2n)	$^{Zn}65$	244 d	11.228
	(n, γ)	$^{Zn}69m$	13.8 h	0
	(n, α)	$^{Ni}65$	2.52 h	0
Zr	(n,2n)	$^{Zr}89$	78.4 h	12.103
	(n,p)	$^{Y}90m$	3.19 h	1.513
	(n,p)	$^{Y}91m$	49.7 min	0.770
	(n,p)	$^{Y}94$	18.7 min	4.180
US Coins		$^{Ni}57$	35.6 h	12.429
		$^{Co}57$	271.8 d	6.051
Stainless Steel		$^{Ni}57$	35.6 h	12.429
		$^{Co}57$	271.8 d	6.051
		$^{Cr}51$	27.7 d	0

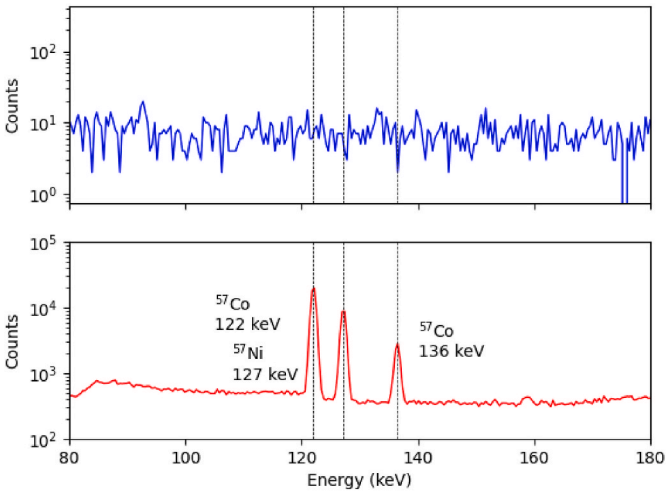

Fig. 1. Nickel target measured with Detector 2 3.67 days after irradiation displaying the 3 MeV gamma ray spectrum (blue) and the 14 MeV gamma spectrum (red). (For interpretation of the references to colour in this figure legend, the reader is referred to the Web version of this article.)

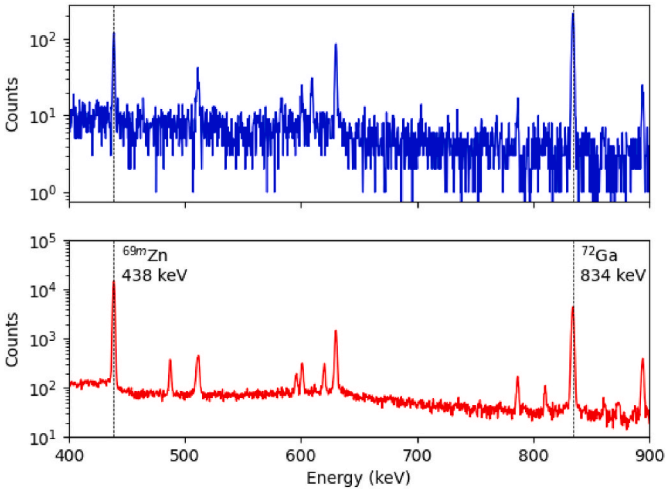

Fig. 2. Gallium target measured with Detector 3 21.5 hours after irradiation displaying both 3 (blue) and 14 (red) MeV spectra. (For interpretation of the references to colour in this figure legend, the reader is referred to the Web version of this article.)

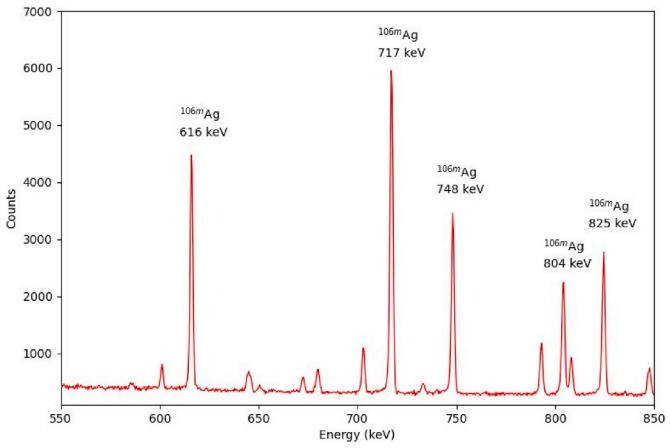

Fig. 3. Silver target measured with Detector 1 9.77 days after the 14-MeV irradiation.

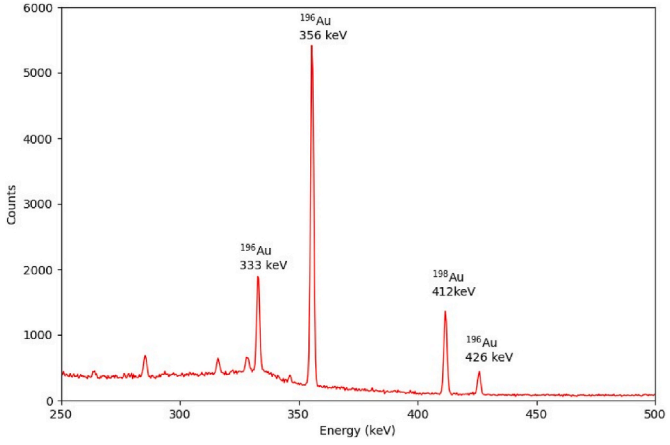

Fig. 4. Gold target measured with Detector 3 1.29 days after the 14-MeV irradiation. (For interpretation of the references to colour in this figure legend, the reader is referred to the Web version of this article.)

5. Conclusions

From the gamma ray spectra we collected following approximately 3 and 14 MeV neutron irradiations of 29 different materials, we have identified 8 that show marked differences in the radioisotopes produced at these two energies. Through the collection and gamma-ray counting of such activated materials following a nuclear explosion, these materials could be used to infer whether it was a pure fission or a fission/fusion weapon. Although we sincerely hope there is no need for this information to be used in the future, we believe it is useful to know that there are in fact ways to infer information about the nature of the weapon from neutron activation of ubiquitous materials.

Declaration of competing interest

The authors declare that they have no known competing financial interests or personal relationships that could have appeared to influence the work reported in this paper.

Acknowledgements

This material is based upon work supported by the Department of Energy National Nuclear Security Administration under Award Number (s) DE-NA0000979 and by the Director, Office of Energy Research, Office of High Energy and Nuclear Physics, Division of Nuclear Physics, of the US De-partment of Energy under Contract No. DE-AC02-05CH11231. We wish to thank the staff of LBNL's 88-Inch Cyclotron for their assistance in these measurement.

References

Beddingfield, D., Cecil, F., 1998. Identification of fissile materials from fission product gamma-ray spectra. Nucl. Instrum. Methods Phys. Res. Sect. A Accel. Spectrom. Detect. Assoc. Equip. 417, 405–412. https://doi.org/10.1016/S0168-9002(98)00781-5. https://www.sciencedirect.com/science/article/pii/S01689002 9_8007815.

Chu, S.Y., Ekström, L.P., Firestone, R.B., 1999. The lund/lbnl nuclear data search. URL: http://nucleardata.nuclear.lu.se/toi/.

Hecker, S.S., 2000. Plutonium and its alloys : from atoms to microstructure. Los Alamos Sci. 26, 290–335. URL: https://library.lanl.gov/cgi-bin/getfile?00818035.pdf.

Hollas, C., Close, D., Moss, C., 1987. Analysis of fissionable material using delayed gamma rays from photofission. In: Nuclear inStruments and Methods in Physics Research Section B: Beam Interactions with Materials and Atoms, vols. 24–25, pp. 503–505. URL: https://www.sciencedirect.com/science/article/pii/0168583X879_06951.

Iyengar, A., Norman, E., Howard, C., Angell, C., Kaplan, A., Ressler, J., Chodash, P., Swanberg, E., Czeszumska, A., Wang, B., Yee, R., Shugart, H., 2013. Distinguishing fissions of 232th, 237np and 238u with beta-delayed gamma rays. In: Nu- Clear Instruments and Methods in Physics Research Section B: Beam Interactions with Materials and Atoms, vol. 304, pp. 11–15. https://doi.org/10.1016/j.nimb.2013.03.054. URL: https://www.sciencedirect.com/science/article/pii/S0168583X13_003893.

Marrs, R., Norman, E., Burke, J., Macri, R., Shugart, H., Browne, E., Smith, A., 2008. Fission-product gamma-ray line pairs sensitive to fissile material and neutron energy. In: Nuclear Instruments and Methods in Physics Research Section A: Accelerators, Spectrom- Eters, Detectors and Associated Equipment, vol. 592, pp. 463–471. URL: https://www.sciencedirect.com/science/article/pii/S0168900208_006463.

Meulders, J.P., Leleux, P., Macq, P.C., Pirart, C., 1975. Fast neutron yields and spectra from targets of varying atomic number bombarded with deuterons from 16 to 50 MeV (for radiobiology and radiotherapy). Phys. Med. Biol. 20, 235–243. https://doi.org/10.1088/0031-9155/20/2/005. URL:

Mint, @U.S., 2021. @Circulating coins.@United States mint. URL: https://www.usmint.gov/learn/coin-and-medal-programs/circulating-coins?action=CircQuarterDollar.

Pritychenko, B., Sonzogni, A., 2021. @Q-value calculator (qcalc). @URL: https://www.nndc.bnl.gov/qcalc/.

Swanberg, E., Norman, E.B., Shugart, H., Prussin, S.G., Browne, E., 2009. Using low resolution gamma detectors to detect and differentiate 239Pu and 235U fissions. J. Radioanal. Nucl. Chem. 282, 901. https://doi.org/10.1007/s10967-009-0283-4.